Conserved methylation signature accurately predicts heavily irradiated CNS tumour with perplexing histopathology: A case report

HANDOKO[1], EKA SUSANTO[2], RENINDRA ANANDA AMAN[3], TIARA ANINDITHA[4], HERI WIBOWO[5], TIARA BUNGA MAYANG PERMATA[1] and SOEHARTATI A. GONDHOWIARDJO[1]

[1]Department of Radiation Oncology, Faculty of Medicine, Cipto Mangunkusumo National General Hospital, University of Indonesia, Jakarta 10430, Indonesia; [2]Department of Anatomical Pathology, Faculty of Medicine, Cipto Mangunkusumo National General Hospital, University of Indonesia, Jakarta 10430, Indonesia; [3]Department of Neurosurgery, Cipto Mangunkusumo National General Hospital, Faculty of Medicine, University of Indonesia, Jakarta 10430, Indonesia; [4]Department of Neurology, Cipto Mangunkusumo National General Hospital, Faculty of Medicine, University of Indonesia, Jakarta 10430, Indonesia; [5]Integrated Laboratory, Faculty of Medicine, University of Indonesia, Jakarta 10430, Indonesia

Received December 31, 2024; Accepted June 18, 2025

DOI: 10.3892/br.2025.2043

Abstract. Diagnosing central nervous system (CNS) tumours post-radiation therapy is often complicated by treatment-induced histological changes. Molecular diagnostics, such as methylation profiling, offer robust tools to aid in accurate tumour classification. The present study reported a case of a 48-year-old woman with a recurrent parasellar mass previously treated with stereotactic radiosurgery. Despite imaging suggestive of meningioma, histopathology and immunohistochemistry yielded ambiguous findings. Low-coverage whole genome methylation profiling using Oxford Nanopore sequencing provided a conclusive diagnosis of meningioma, with a classifier confidence score of 0.791, supported by t-distributed stochastic neighbor embedding clustering and characteristic copy number variations. The present case illustrated the diagnostic utility of methylation profiling in post-treatment CNS tumours with perplexing histopathology. Integration of molecular diagnostics can enhance classification accuracy and inform clinical decision-making.

Introduction

The diagnosis of central nervous system (CNS) tumours has evolved significantly over the past decade, moving beyond traditional clinical and histopathological assessments to an integrated, multi-dimensional approach that incorporates molecular diagnostics (1). The 2021 WHO classification of CNS tumours introduced a paradigm shift by emphasizing the need for a molecularly informed diagnosis that combines histopathological findings with specific genetic, epigenetic, and protein expression profiles (2,3). This integrated diagnosis framework allows for more accurate tumour classification, as numerous CNS tumours exhibit overlapping histological features but distinct molecular signatures that directly impact prognosis and therapeutic decisions.

Immunohistochemistry (IHC) remains a cornerstone for initial tumour characterization, providing insights into cellular lineage and differentiation. However, it often falls short in cases with ambiguous morphology or treatment-induced changes. Next-generation sequencing (NGS) technologies, such as targeted gene panels, whole-exome sequencing, and methylation profiling, are increasingly essential to identify diagnostic, prognostic, and therapeutic markers. For example, the detection of specific mutations (such as IDH1/2 in gliomas, BRAF V600E in gangliogliomas or pleomorphic xanthoastrocytomas), chromosomal alterations (such as 1p/19q co-deletion in oligodendrogliomas), or methylation patterns [such as O^6-methylguanine-DNA methyltransferase (MGMT) promoter methylation or genome-wide methylation classifiers] is now pivotal in classifying CNS tumours (2). This molecular classification not only refines diagnostic accuracy but also provides critical information on tumour behaviour, treatment response, and patient outcomes, underscoring the necessity for a comprehensive, integrated diagnostic approach in modern neuropathology (4).

The accurate diagnosis of CNS tumours is the most challenging for cases that have been previously treated. Tumours subjected to pre-treatment modalities such as radiation or chemotherapy frequently undergo morphological and molecular changes that can obscure their histopathological features. This phenomenon, known as treatment-related distortion, complicates subsequent diagnostic efforts,

Correspondence to: Dr Tiara Bunga Mayang Permata or Soehartati A. Gondhowiardjo, Department of Radiation Oncology, Faculty of Medicine, Cipto Mangunkusumo National General Hospital, University of Indonesia, Jakarta 10430, Indonesia
E-mail: dr.mayangpermata@gmail.com
E-mail: gondhow@gmail.com

Key words: central nervous system tumour, methylation profiling, radiation, meningioma, molecular diagnostics, nanopore sequencing

making it difficult to discern between tumour recurrence, radiation-induced changes, or an entirely new entity (5). For instance, gliomas, such as high-grade gliomas, often exhibit post-radiation changes including nuclear and cytoplasmic enlargement, which may also mimic pseudo-malignant radiation-associated changes (6). Similarly, meningiomas post-irradiation may exhibit increased cellular atypia, loss of classic whorl patterns, and elevated Ki-67 indices reflecting either radiation-induced proliferation or cell death (7). These changes can mimic features of higher-grade malignancies, leading to diagnostic uncertainty when relying solely on histopathology and IHC.

Post-treatment CNS tumours, especially those subjected to high-dose radiation, pose a significant diagnostic dilemma due to treatment-related changes. Recurrent CNS tumours exhibit histopathological features altered by prior therapies, complicating differentiation between tumour recurrence, treatment-induced necrosis, or secondary malignancies (8-10) For instance, a 2023 study by Wood *et al* (5) highlighted that paediatric high-grade astrocytoma post-treatment showed increased tumour mutation burden and morphological ambiguity in a subset of recurrences, underscoring the prevalence of diagnostic challenges (5). Similarly, radiation-induced changes, such as fibrosis, vascular alterations, and cellular atypia, can mimic aggressive tumour features, leading to misclassification rates as high as 20% when relying solely on histopathology and IHC (11). IHC, while valuable for initial tumour characterization, often yields inconclusive or conflicting results in these cases due to altered protein expression profiles induced by therapy.

Recent advances in epigenomic profiling, such as whole genome methylation profiling, have emerged as potent tools for resolving such diagnostic dilemmas (12,13). Unlike protein expression or histopathological features, which are highly susceptible to treatment-induced alterations, DNA methylation patterns exhibit high stability, even in the presence of morphological distortions. This stability arises because DNA methylation, an epigenetic modification, is regulated by DNA methyltransferases and remains relatively unaffected by the cellular stress or protein turnover induced by therapies such as radiation, whereas downstream protein expression is disrupted by changes in transcription, translation, or protein degradation pathways (14). For example, radiation may upregulate stress-response genes or silence tumour suppressor genes via histone modifications, altering IHC-detectable proteins such as p53 or mucin 1, cell surface associated (EMA), while the underlying CpG methylation patterns at promoter regions remain conserved (15). This phenomenon has been reported in brain malignancies; a study on recurrent glioblastomas demonstrated that methylation profiles of MGMT were preserved despite chemoradiation (16). This was likely because promoter methylation is relatively stable, and does not require active maintenance of methylation status by DNA methyltransferases (DNMTs) (17).

Methylation profiling leverages this conserved epigenetic signature to provide robust molecular classification, offering a distinct advantage over existing methodologies. Methylation profiling can provide a rigorous molecular classification that remains largely unaffected by histopathological distortions. In the present study, a case of a patient with a heavily irradiated CNS tumour that exhibited perplexing histological features, making definitive diagnosis difficult, is reported. Despite extensive immunohistochemical analysis, the tumour remained unclassifiable. To address this diagnostic impasse, low-coverage whole genome methylation profiling, a technique that has shown promise in accurately predicting the molecular subtype of various cancers, even in the presence of histological ambiguity, was employed.

Case report

Patient information. A clinical sample was obtained from a patient 48-year-old female who initially presented with a parasellar mass, clinically resembling an extra-axial tumour. An initial MRI performed in December 2022 revealed a 3.6x4.3x3.1 cm tumour in left parasellar region, raising suspicion for meningioma or craniopharyngioma (Fig. 1A). The patient initially declined surgical intervention and was instead treated with Gamma Knife stereotactic radiosurgery, receiving a dose of 14 Gy in December 2022. Subsequent MRI follow-ups were conducted every six months. The tumour remained stable in size for up to one year post-radiation, as shown in MRI scans from June 2023 and December 2023 (Fig. 1B and C, respectively). After ~1 year and 3 months post-radiation treatment, a brain MRI performed in March 2024 revealed a progressive tumour at the same location extending to the left cerebellopontine angle and abutting the brainstem (Fig. 1D). Surgery was offered and the patient agreed. A subtotal resection was performed in March 2024; however the surgeon was unable to achieve gross total resection due to the tumour encasing the cavernous sinus. At the follow-up 6 months after the surgery, the patient did not exhibit any significant symptoms, and an MRI scan performed in October 2024, revealed stable disease (Fig. 1E). An MRI was performed again 6 months later in April 2025 and revealed a slight reduction of tumour size (Fig. 1F). Since there was no progression of disease, no further intervention was undertaken.

A tissue sample was obtained during craniotomy performed in in March 2024 from the left retroclival region. Histopathological analysis and further immunohistochemical assessment performed in April 2024 were both inconclusive; therefore, further molecular examination was performed. Ethical clearance was obtained from the Ethics Committee of the Faculty of Medicine, University of Indonesia (Jakarta, Indonesia) in accordance with the Declaration of Helsinki, for the collection and molecular testing of biological specimens from rare and recurrent tumours at any site. Written informed consent was obtained from the patient prior to molecular testing, ensuring full disclosure of the purpose, procedures and potential use of biological specimens for research in the present study. The specimen was retrieved from the Department of Pathology of Cipto Mangunkusumo National General Hospital (Jakarta, Indonesia) in the form of formalin-fixed paraffin-embedded (FFPE) tissue. DNA extraction was performed on the FFPE tissue sample, followed by NGS sequencing using a third generation sequencing platform, and the methylation profile was analysed. The DNA extraction and NGS were performed in August 2024. The molecular information was then matched with available

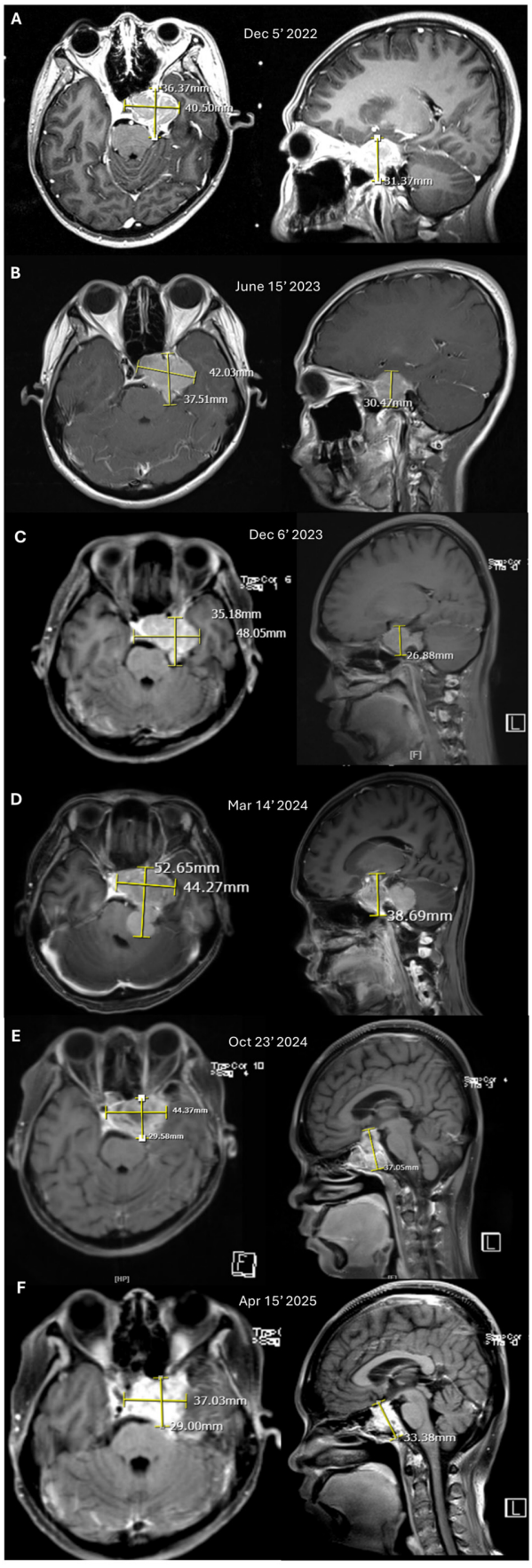

Figure 1. T1 contrast-enhanced brain magnetic resonance imaging revealing the parasellar lesion in axial and sagittal sections (A) before SRS, (B) 6 months post-SRS, (C) 12 months post-SRS, (D) 18 months post-SRS, (E) 6 months post-surgery and (F) 1 year post-surgery. SRS, stereotactic radiosurgery

clinical, imaging, histopathology and immunohistochemcial results.

Tissue processing and IHC. The tumour tissue sample was initially fixed in 10% neutral buffered formalin for 24 at 4˚C to preserve cellular structure and protein antigenicity, followed by dehydration and embedding in paraffin wax. Once embedded, the tissue was sectioned into thin slices with a thickness of 4-5 μm using a microtome, and was then mounted onto positively charged glass slides to ensure optimal adherence. The slides were baked at 60˚C to solidify tissue attachment before further processing. The next step was deparaffinization and rehydration. Tissue sections were deparaffinized by immersing them in xylene, followed by rehydration through a graded series of ethanol solutions of decreasing concentrations (100, 95 and 70%) and finally in distilled water. To expose the antigenic sites, antigen retrieval was performed using a heat-induced epitope retrieval (HIER) technique in an EDTA buffer (pH 9.0). This step resulted in unmasking the target epitopes and enhancing antibody binding.

Following antigen retrieval, non-specific binding was minimized by incubating the slides with a blocking solution, 10% bovine serum albumin (cat. no. 37520; Thermo Fisher Scientific, Inc.) for 30 min at room temperature. After blocking, primary antibodies (Table I) specific to each target protein marker were applied at their optimized dilutions following each antibody kit manufacturer guideline. The slides were then incubated in a humid chamber for 2 h at room temperature. This step enabled the primary antibodies to bind specifically to their corresponding antigens in the tissue sections. The detection of bound primary antibodies was carried out using an appropriate secondary antibody conjugated to a biotin enzyme, horseradish peroxidase (HRP) (mouse anti-human IgG4 Fc, secondary antibody, HRP; 1:1,000; cat. no. A-10654; Thermo Fisher Scientific, Inc.) for 1 h at room temperature. A chromogenic substrate, 3,3'-diaminobenzidine (DAB), was used to develop a brown colour, indicating the presence of the target antigen. Counterstaining with hematoxylin was performed for 5 min at room temperature to provide contrast by staining cell nuclei blue, aiding in the morphological assessment of the tissue.

After staining, the slides underwent a series of dehydration steps using graded alcohols, followed by clearing in xylene, and were finally mounted with a permanent mounting medium. The prepared slides were then examined under a light microscope by a senior neuropathologist to evaluate the expression patterns of the specific markers. The staining intensity and proportion of positive cells were recorded for each marker. The immunohistochemical markers examined were Vimentin, AE1/3, EMA, p63, S100, PR, CD34, Ki-67, p40, CK7, CK8, HMWCK, Cam5.2, CK20, ER, STAT6, TTF-1, BRAF V600E, β-catenin, TLE-1, BCL2, CD99, and CD56.

DNA extraction. The DNA extraction of the FFPE tissue was carried out using the QIAamp DNA FFPE Tissue Kit (cat. no. 56404; QIAGEN) which involved several key steps. Initially, the FFPE tissue sample was deparaffinized using a xylene and ethanol wash to remove any residual paraffin. Then the tissue was prepared for next process, lysis. This lysis

Table I. Antibodies for immunohistochemical staining.

Immunohistochemical marker	Supplier	Cat. no.	Dilution
Vimentin	Leica Biosystems	PA0640	RTU
AE1/3	Leica Biosystems	PA0909	RTU
EMA	Leica Biosystems	NCL-L-EMA	1:400
p63	Biocare Medical, LLC	CM163C	1:50
S100	Biocare Medical, LLC	ACR3237C	1:200
Synaptophysin	Biocare Medical, LLC	CM371C	1:200
Chromogranin	Cell Marque; Merck KGaA	238M-96	1:500
PR	Roche Diagnostics	5277990001	RTU
CD34	BioSB, Inc.	BSB5230	1:100
Ki-67	Roche Diagnostics	5278384001	RTU
p40	BioSB, Inc.	BSB2075	1:200
CK7	BioSB, Inc.	BSB5412	1:600
CK8	BioSB, Inc.	BSB6665	1:100
CK19	Biocare Medical, LLC	CM242C	1:100
HMWCK	BioSB, Inc.	BSB5398	1:50
Cam5.2	Cell Marque; Merck KGaA	452M-96	1:100
CK20	Biocare Medical, LLC	CM062C	1:200
ER	Roche Diagnostics	5278406001	RTU
STAT6	Biocare Medical, LLC	ACI3244C	1:100
TTF-1	Leica Biosystems	PA0364	RTU
BRAF V600E	BioSB, Inc.	BSB2824	1:250
Beta catenin	Biocare Medical, LLC	CM406C	1:200
TLE-1	Cell Marque; Merck KGaA	401M-16	1:100
BCL2	Leica Biosystems	PA0117	RTU
CD99	Cell Marque; Merck KGaA	199R-16	1:100
CD56	Leica Biosystems	NCL-L-CD56-504	1:100

RTU, ready-to-use.

step involved breakdown of the cross-linked proteins in the FFPE samples. The sample underwent incubation with a lysis buffer and proteinase K (both included in the aforementioned kit) to digest the tissue and release the DNA into the solution.

Once lysis was completed, the sample was treated with a heat incubation step up to 90˚C to reverse formalin-induced crosslinking, which helped to ensure optimal DNA recovery and purity. The lysate was then mixed with ethanol and passed through a QIAamp MinElute column, which selectively bonded the DNA. Following several washes to remove contaminants, the purified DNA was eluted in a low-salt buffer, ready for downstream sequencing applications. The authors adhered strictly to the manufacturer-recommended protocol for extracting FFPE tissue. The complete and detailed protocol was available publicly in the corresponding kit documentation online. The extracted DNA was measured for purity using Nanodrop Spectrophotometer and the quantity was measured using Qubit Fluorometers (both from Thermo Fisher Scientific, Inc.).

NGS sequencing. The extracted DNA was sequenced using a third generation sequencer from (Oxford Nanopore Technologies plc). A ligation-based protocol was used to prepare the library DNA [Ligation sequencing DNA V14 (SQK-LSK114); Oxford Nanopore Technologies plc]. There was no PCR step involved to preserve the native methylation information within the DNA. The type of sequencing was direct DNA sequencing with modified bases for methylation detection. The DNA was sequenced using PromethION flow cell (cat. no. FLO-PRO114M; Oxford Nanopore Technologies plc) with chemistry version R 10.4.1. The library loading concentration was 20 fmol and the software used for analysis (basecalling and alignment) was MinKNOW Version 25.02 (Oxford Nanopore Technologies plc). The detailed library preparation and sequencing steps were carried out according to the publicly available Nanopore protocol on the Nanopore Community webpage. The present study aimed to obtain low coverage whole genome sequencing, and thus the sequencing was carried out for 3 h until the raw data in POD5 format reached ~50 GB. The sequencing was then interrupted and stopped. The overview process for molecular testing, from IHC and methylation testing to correlation with clinical and imaging data, is illustrated in Fig. 2.

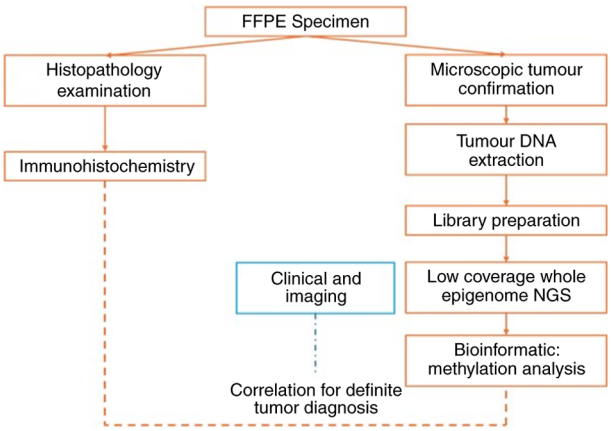

Figure 2. Overview of the molecular testing process through correlation with clinical and imaging data to establish a definite diagnosis. FFPE, formalin-fixed paraffin-embedded; NGS, next-generation sequencing.

Methylation analysis. After sequencing was completed, post-run basecalling was performed using the dna_r10.4.1_e8.2_400bps_sup@v5.0.0 model, which included 5mCG and 5hmCG base modification calling with Dorado (18). The methylation analysis was then carried out using NanoDx pipeline, which is publicly available (12,19). Briefly, the basecalled sequencing reads were aligned to the hg19 human reference genome using Minimap2 (20). Methylation information was then extracted using Modkit version 0.4.0 (https://github.com/nanoporetech/modkit), which provides single-base resolution of methylation data. The methylation matrix was then constructed representing all CpG sites. Furthermore, dimensionality reduction using t-SNE was applied to visualise and analyse the high-dimensional methylation data. The methylation data was classified using the public Heidelberg brain tumour classifier v11b4 reference set (21).

Clinical findings. The histopathology results revealed a tumour mass that under microscopic examination, was arranged in irregular short lines, forming sheets, lobules and a patternless architecture (Fig. 3A). The tumour cells exhibited round to oval nuclei with spindle shapes, mild to moderate pleomorphism, slightly coarse chromatin, and eosinophilic cytoplasm. The mitotic count was 6 per 10 low-power fields. Blood vessels appeared partially congested. There was dense infiltration of macrophages or foamy cells around the tumour. This histopathological feature was inconclusive, with the histology suggesting the possibility of meningioma, solitary fibrous tumour, pituitary adenoma or carcinoma.

IHC was performed and the results obtained from all the tested markers are summarized in Table II, Fig. 3B-H, and Fig. S1. The Ki-67 index of up to 20% was indicative of moderately high proliferative activity, suggesting a potentially aggressive tumour. Positive BRAF V600E expression suggested the presence of this mutation in the tumour, which was also indicative of a more aggressive tumour and poorer prognosis. The findings of IHC indicated partial epithelial and mesenchymal marker expression (Vimentin, AE1/3 and EMA) and BRAF V600E positivity, along with negative markers for neural and neuroendocrine differentiation, suggesting that the tumour may be a type of mixed epithelial-mesenchymal tumour or a variant of glioma or meningioma with complex differentiation. The neuropathologist concluded that this was more likely a craniopharyngioma. The ambiguous

Table II. Results of immunohistochemical analysis.

Immunohistochemical marker	Result
Vimentin	Expressed in most tumour cells
AE1/3	Positive in some tumour cells
EMA	Positive in some tumour cells
p63	Positive in some tumour cells
S100	Negative
Synaptophysin	Negative
Chromogranin	Negative
PR	Negative
CD34	Only expressed in vessel walls
Ki-67	Increased, variable, up to 20% in some areas
p40	Positive in some tumour cells
CK7	Positive in some tumour cells
CK8	Positive in some tumour cells
CK19	Positive in some tumour cells
HMWCK	Positive in some tumour cells
Cam5.2	Positive in some tumour cells
CK20	Negative
ER	Negative
STAT6	Expressed in tumour cells (cytoplasmic reactivity, rather than nucleus)
TTF-1	Negative
BRAF V600E	Positive in most tumour cells
Beta catenin	Cytoplasmic and membranous expression in some tumour cells
TLE-1	Positive in some tumour cells with weak intensity
BCL2	Expressed in some (few) tumour cells
CD99	Weak cytoplasmic and membranous expression in some tumour cells
CD56	Positive in a small number of tumour cells

AE1/3, pan-cytokeratin antibody cocktail; EMA, mucin 1, cell surface associated; p63, tumor protein p63; S100, calcium-binding proteins; PR, progesterone receptor; CD34, cluster of differentiation 34; Ki-67, antigen Kiel 67; p40, ΔNp63 isoform of the p63 protein; CK7, cytokeratin 7; CK19, cytokeratin 19; HMWCK, high molecular weight cytokeratin; Cam5.2, anti-cytokeratin antibody; CK20, cytokeratin 20; ER, estrogen receptor; STAT6, signal transducer and activator of transcription 6; TTF-1, thyroid transcription factor-1; BRAF V600E, B-Raf proto-oncogene, serine/threonine kinase, with V600E mutation (Val600Glu); TLE-1, transducin-like enhancer of split 1; BCL2, B-cell lymphoma 2; CD99, cluster of differentiation 99; CD56, cluster of differentiation 56.

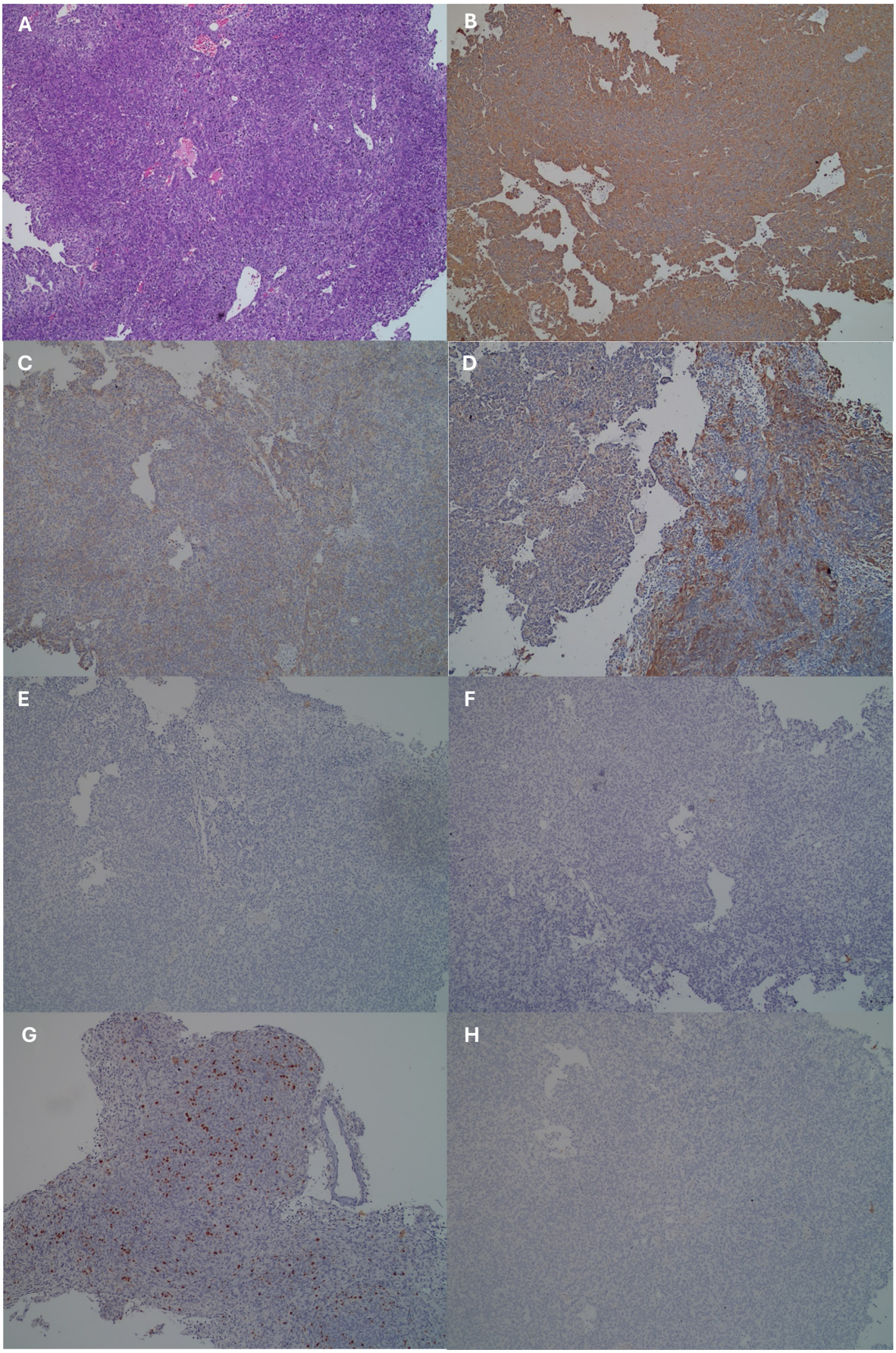

Figure 3. Histopathology and immunohistochemical findings. (A) Haematoxylin and eosin staining. (B-H) Immunohistochemical staining of the following markers: (B) Vimentin, (C) EMA, (D) AE1/3, (E) S100, (F) PR, (G) Ki-67 and (H) synaptophysin. All images were obtained at a magnification of x100. EMA, mucin 1, cell surface associated. EMA, mucin 1, cell surface associated; AE1/3, pan-cytokeratin antibody cocktail; S100, calcium-binding proteins; PR, progesterone receptor.

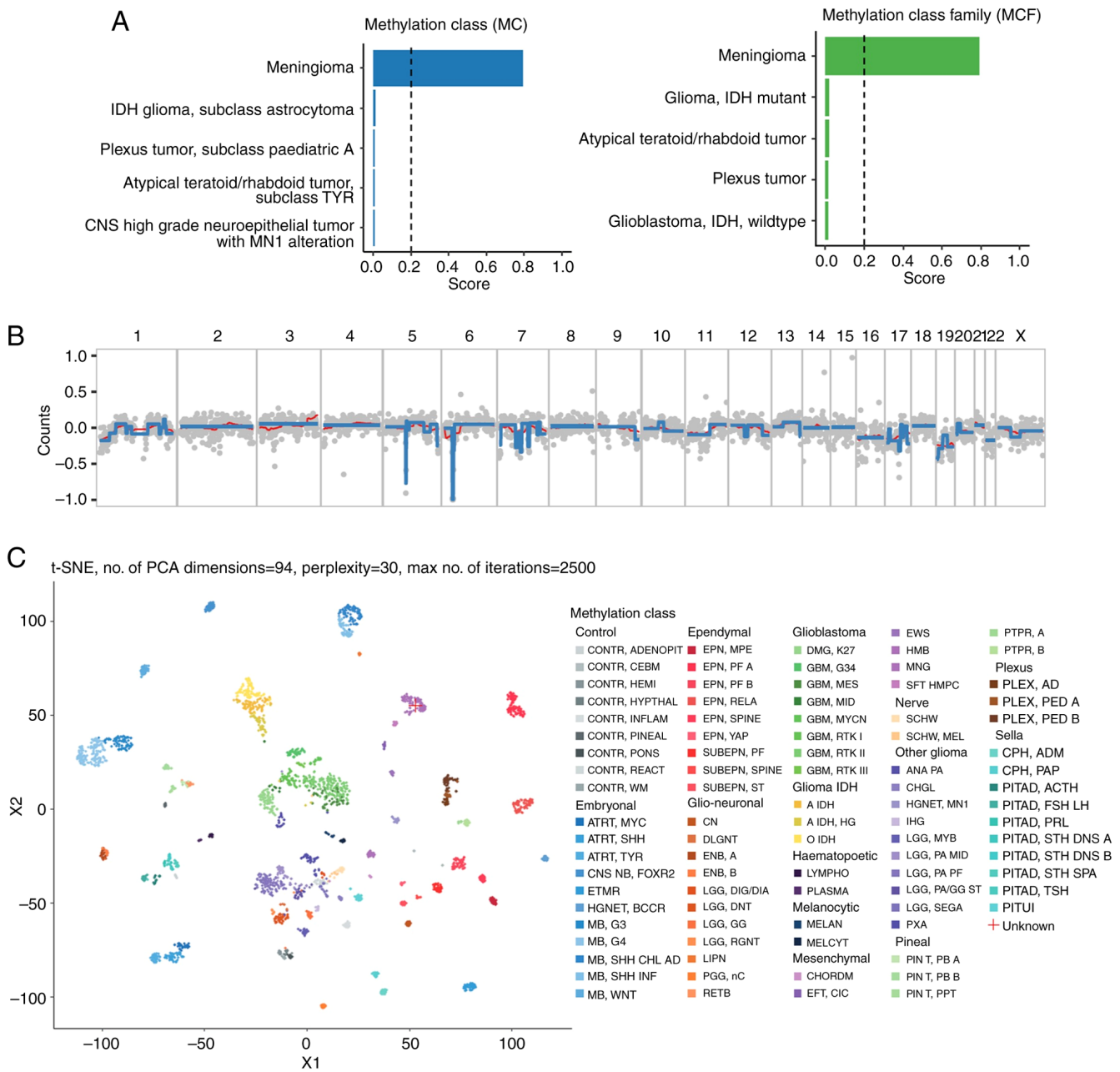

Figure 4. Methylation classification results. (A) Methylation class and methylation class family assignements, (B) low-coverage copy number variation profile and (C) t-SNE clustering map demonstrating clustering consistent with meningioma.

morphological findings on the histopathology and atypical expression were likely due to prior high-dose stereotactic radiotherapy to the tumour. Based on the histopathology and immunohistochemical results alone, a definitive classification could not be made; however, the most likely diagnosis was craniopharyngioma.

Further molecular analysis was performed using NGS to conduct direct sequencing in order to detect random whole genome methylation from the tumour DNA. The methylation classification analysis of the CNS tumour sample identified the tumour as a meningioma at both the methylation class and methylation class family levels. The confidence score for this classification was 0.791, which was above the commonly used threshold of 0.2, indicating a reliable prediction. The Heidelberg classifier, validated in large cohorts, demonstrates a sensitivity of 92-95% and specificity of 90-93% for meningioma classification in untreated cases (22-24), although its performance in irradiated tumours remains less well studied. In this context, the 0.791 score suggests reliable discrimination despite post-treatment complexity. This results suggested that the epigenetic profile of the tumour was most consistent with meningioma when compared to the reference profiles of CNS tumours. Additionally, the classification was supported by the absence of strong signals for other CNS tumour entities among the top five categories, which included high-grade neuroepithelial tumours, atypical teratoid/rhabdoid tumours, and various gliomas (Fig. 4A).

The copy number variation (CNV) profile, shown in Fig. 4B, was generated based on low-coverage whole genome

sequencing data. Due to the low coverage, the resolution of the CNV analysis may be limited, and fine-scale alterations could be missed. Nonetheless, it provided an overview of the broader chromosomal changes present in the tumour specimen. Overall, the CNV plot revealed regions with potential copy number gains (positive log2 values represented by red bars) and losses (negative log2 values represented by blue bars) across multiple chromosomes. The copy number profile showed relative stability across most chromosomes, with the majority of regions falling within the-0.5 to 0.5 range on the y-axis, indicating no major large-scale chromosomal gains or losses.

Chromosome 5 and 6 exhibited large segments of copy number loss, indicating possible deletions. A slight gain was visible on the q arm of chromosome 1, extending approximately from the middle to the end of the chromosome. The 1q gain observed in the copy number profile was consistent with the classification of a meningioma, as gain of 1q is a known recurrent alteration in certain meningioma subtypes (25). Chromosome 22 had a noticeable deletion, which was consistent with known chromosomal patterns in meningiomas (26,27). Despite the lower resolution of this analysis, these broad CNV changes provide valuable insights into the overall genomic landscape of the tumour and could serve as a preliminary indicator for further validation using higher-coverage sequencing methods.

The dimensionality reduction plot further corroborated this classification by visually clustering the sample close to the meningioma reference group, distinct from other tumour classes such as glioblastomas or embryonal tumours (Fig. 4C). This visualization tool, while only qualitative, reinforces the classification outcome by showing that the methylation pattern of the sample overlaps predominantly with meningioma profiles. Given the relatively high number of CpG sites used in the classification (11,653 sites), the prediction was considered robust, as it comprehensively covered relevant loci for distinguishing CNS tumour types. A final diagnosis was obtained following multidisciplinary assessment of all available data, and considered this entity to be a meningioma. Compared with IHC, which required 5-10 days and yielded inconclusive results, methylation profiling provided a definitive diagnosis in 4-7 days (from DNA extraction to classification), with an estimated accuracy of >90% based on classifier benchmarks (21,23,24). This quantitative advantage highlights the superiority of methylation profiling in both speed and diagnostic precision, particularly in complex cases.

Discussion

The present case report highlights the complexities encountered in diagnosing CNS tumours post-radiation therapy. The patient's initial clinical presentation and radiological features were consistent with a meningioma. However, following Gamma Knife treatment and subsequent tumour recurrence, the histopathological and immunohistochemical profiles suggested craniopharyngioma, a diagnosis with a vastly different therapeutic approach. The discordance between clinical and pathological findings was likely attributable to radiation-induced histological alterations (28).

The immunohistochemical result of the proliferation marker Ki-67 showed increased expression in some areas, reaching up to 20%, indicative of a moderate proliferative index, which suggests an intermediate to high level of tumour aggressiveness. The positive BRAF V600E expressed in a substantial portion of tumour cells was extremely rare in meningioma, even in grade 3 meningioma (29). It is commonly mutated in certain gliomas, gangliogliomas and melanomas (30). The presence of the BRAF V600E mutation is associated with more aggressive behavior in certain types of cancer (31). In this case, the mutation was likely acquired secondararily following radiation therapy. Based on the immunohistochemical profile, it was unlikely to be a meningioma.

The discordance between clinical, imaging, histopathology and immunohistochemical findings hindered appropiate management of the patient. Such cases underscore the limitations of conventional histopathology and IHC, in the context of previously treated tumours. Radiation can induce both morphological and molecular changes, including altered expression of key diagnostic markers. This phenomenon poses a significant challenge in distinguishing true recurrence from treatment-related effects.

Methylation profiling emerged as a critical diagnostic tool in this scenario, providing a definitive classification based on the intrinsic epigenetic landscape of the tumour. The methylation profile has been shown to be conserved between primary and metastatic samples (32), although the driver mutations may differ. Evidence from ovarian cancer, which is often heavily treated with chemotherapeutic agents and prone to recurrance, has shown that the methylation signature is preseerved between primary and recurrent tumours (33).

Meningioma methylation profiles typically exhibit hypermethylation at HOX gene clusters and hypomethylation at cell cycle regulatory genes, distinguishing them from other CNS tumours (34,35). For comparison, glioblastomas exhibit widespread hypomethylation of oncogenes such as EGFR and hypermethylation of tumour suppressor genes such as MGMT, patterns that correlate with aggressive proliferation and resistance to therapy (16,36,37). Craniopharyngiomas, initially suspected in this case, display distinct WNT/β-catenin pathway activation, linked to their epithelial differentiation and cystic growth patterns (38-40). In this case, the absence of WNT pathway activation, evidenced by negative β-catenin staining, aided in ruling out craniopharyngioma.

While meningioma methylation signatures are often correlated with the risk of recurrence (such as hypermethylation at NF2 in aggressive subtypes) (41), physiological associations in irradiated cases remain underexplored due to limited post-treatment data. A definitive link between the observed methylation patterns and specific physiological traits such as proliferation or invasiveness could not be established, as this would require functional studies which were beyond the scope of the present work. However, the conserved methylation profile observed despite prior radiation, aligns with evidence from other cancers, such as ovarian cancer, where methylation signatures remain stable between primary and recurrent tumours despite treatment (33).

Moreover, the copy number profile did not show any substantial deviations that would suggest chromosomal

aberrations typical of more aggressive gliomas or embryonal tumours, which often present with distinct copy number alterations (36). This finding aligns with the relatively stable genomic profile typically observed in meningiomas, especially in non-anaplastic forms. Collectively, these findings provide a strong molecular basis for classifying the sample as a meningioma, with implications for the prognosis of the patient and potential therapeutic strategies.

The identification of a meningioma-specific methylation signature was pivotal in resolving the present case. With a conclusive diagnosis of meningioma, it is now understood that gross total resection should be pursued in the event of recurrence, an approach not typically required in cases of craniopharyngioma. This demonstrated the utility of methylation profiling as a complementary diagnostic approach for challenging CNS tumours. Incorporating such advanced molecular techniques into routine diagnostics can enhance the accuracy of CNS tumour classification, particularly for complex cases where conventional methods fall short (42). Adopting methylation profiling as a standard in neuro-oncology could transform diagnostics, particularly for recurrent CNS tumours with treatment-altered histopathology. Unlike targeted gene panels, which focus on specific mutations (such as IDH1/2) and may miss broader epigenetic context, or RNA sequencing, which is sensitive to RNA degradation in FFPE samples (43), methylation profiling offers a stable, genome-wide view of tumor biology (44). Therefore, methylation profiling can outperform gene panels in classifying ambiguous cases and is more robust than RNA sequencing in post-treatment settings.

Cost-effectiveness is a key consideration. While the initial setup cost for NGS platforms such as Oxford Nanopore exceeds IHC, the improved diagnostic accuracy can reduce downstream costs from misdiagnosis or unnecessary treatments, potentially saving thousands of dollars per patient. Barriers to implementation include limited access to equipment, the need for specialized technical expertise, poor DNA quality of FFPE samples for NGS, and challenges integrating these methods into clinical workflows, particularly in resource-limited settings. However, declining sequencing costs, improved NGS technology, and scalable protocols (such as low-coverage approaches) could mitigate these challenges. Overall, the analysis of the present study highlighted the utility of methylation profiling in providing a precise, molecular-based classification of CNS tumours, particularly in cases where histopathological evaluation may be challenging. The integration of methylation data with genomic information, as demonstrated in the present study, is critical in the context of CNS tumours, where the accurate classification can directly influence clinical decision-making and patient management strategies. In conclusion, methylation signatures can provide a robust, treatment-resistant classification method, offering clarity in diagnostically challenging cases and guiding appropriate therapeutic strategies. Future research should focus on expanding the CNS methylation classifier to include post-treatment profiles, validating its utility across diverse tumour types, and assessing long-term outcomes of methylation-guided management. Standardizing protocols and addressing cost barriers will further enhance its integration into routine diagnostics, improving patient outcomes in complex neuro-oncology cases.

Acknowledgements

Not applicable.

Funding

The present case report was supported by the PUTI grant from the University of Indonesia (grant no. NKB-412/UN2.RST/HKP.05.00/2023).

Availability of data and materials

The data generated in the present study may be found in the SRA database under accession no. PRJNA1240044 (SRA accession no. SRR32801446) or at the following URL: https://dataview.ncbi.nlm.nih.gov/object/PRJNA1240044?reviewer=hgbuness2eea3b45vlvo9bb134.

Authors' contributions

H contributed to the conceptualization, methodology, investigation, formal analysis, and writing of the original draft. ES contributed to acquisition of data, visualization and the writing, review and editing of the manuscript. RA contributed to conceptualization, resources, investigation, as well as the writing, review and editing of the manuscript. TA contributed to the conceptualization, investigation, as well as the writing, review and editing of the manuscript. HW contributed to the interpretation of data, obtaining resources, project administration, as well as the writing, review and editing of the manuscript. TBMP contributed to the conceptualization and funding acquisition, as well as the writing, review and editing of the manuscript. SAG contributed to the conceptualization, supervision, obtaining resources, and funding acquisition, as well as the writing, review and editing of the manuscript. H and ES confirm the authenticity of all the raw data. All authors contributed equally to this study, and have read and approved the final manuscript.

Ethics approval and consent to participate

The present study was performed in line with the principles of the Declaration of Helsinki. Approval (ethics approval no. KET-289/UN2.F1/ETIK/PPM.00.02/2024) was granted by the Ethics Committee of the University of Indonesia (Jakarta, Indonesia). Written informed consent was secured from the patient prior to molecular testing, ensuring full disclosure of the study's purpose, procedures, and potential use of biological specimens for research.

Patient consent for publication

Written informed consent was secured from the patient prior to molecular testing for the use of any patient data or associated images.

Competing interests

The authors declare that they have no competing interests.

References

1. Kristensen BW, Priesterbach-Ackley LP, Petersen JK and Wesseling P: Molecular pathology of tumors of the central nervous system. Ann Oncol 30: 1265-1278, 2019.
2. Louis DN, Perry A, Wesseling P, Brat DJ, Cree IA, Figarella-Branger D, Hawkins C, Ng HK, Pfister SM, Reifenberger G, *et al*: The 2021 WHO classification of tumors of the central nervous system: A summary. Neuro Oncol 23: 1231-1251, 2021.
3. Smith HL, Wadhwani N and Horbinski C: Major features of the 2021 WHO classification of CNS tumors. Neurotherapeutics 19: 1691-1704, 2022.
4. Singer LS, Feldman AZ, Buerki RA, Horbinski CM, Lukas RV and Stupp R: The impact of the molecular classification of glioblastoma on the interpretation of therapeutic clinical trial results. Chin Clin Oncol 10: 38, 2021.
5. Wood MD, Beadling C, Neff T, Moore S, Harrington CA, Baird L and Corless C: Molecular profiling of pre- and post-treatment pediatric high-grade astrocytomas reveals acquired increased tumor mutation burden in a subset of recurrences. Acta Neuropathol Commun 11: 143, 2023.
6. Ng WK: Radiation-associated changes in tissues and tumours. Curr Diagn Pathol 9: 124-136, 2003.
7. Umekawa M, Shinya Y, Hasegawa H, Morshed RA, Katano A, Shinozaki-Ushiku A and Saito N: Ki-67 labeling index predicts tumor progression patterns and survival in patients with atypical meningiomas following stereotactic radiosurgery. J Neurooncol 167: 51-61, 2024.
8. Verma N, Cowperthwaite MC, Burnett MG and Markey MK: Differentiating tumor recurrence from treatment necrosis: A review of neuro-oncologic imaging strategies. Neuro Oncol 15: 515-534, 2013.
9. Smith EJ, Naik A, Shaffer A, Goel M, Krist DT, Liang E, Furey CG, Miller WK, Lawton MT, Barnett DH, *et al*: Differentiating radiation necrosis from tumor recurrence: A systematic review and diagnostic meta-analysis comparing imaging modalities. J Neurooncol 162: 15-23, 2023.
10. Cacciotti C, Lenzen A, Self C and Pillay-Smiley N: Recurrence patterns and surveillance imaging in pediatric brain tumor survivors. J Pediatr Hematol Oncol 46: e227-e232, 2024.
11. Lebrun L, Gilis N, Dausort M, Gillard C, Rusu S, Slimani K, De Witte O, Escande F, Lefranc F, D'Haene N, *et al*: Diagnostic impact of DNA methylation classification in adult and pediatric CNS tumors. Sci Rep 15: 2857, 2025.
12. Kuschel LP, Hench J, Frank S, Hench IB, Girard E, Blanluet M, Masliah-Planchon J, Misch M, Onken J, Czabanka M, *et al*: Robust methylation-based classification of brain tumours using nanopore sequencing. Neuropathol Appl Neurobiol 49: e12856, 2023.
13. Park JW, Lee K, Kim EE, Kim SI and Park SH: Brain tumor classification by methylation profile. J Korean Med Sci 38: e356, 2023.
14. Lyko F: The DNA methyltransferase family: A versatile toolkit for epigenetic regulation. Nat Rev Genet 19: 81-92, 2018.
15. Lee TG, Kim SY, Kim HR, Kim H and Kim CH: Radiation induces autophagy via histone H4 lysine 20 trimethylation in non-small cell lung cancer cells. Anticancer Res 40: 2537-2548, 2020.
16. Brandes AA, Franceschi E, Paccapelo A, Tallini G, De Biase D, Ghimenton C, Danieli D, Zunarelli E, Lanza G, Silini EM, *et al*: Role of MGMT methylation status at time of diagnosis and recurrence for patients with glioblastoma: Clinical implications. Oncologist 22: 432-437, 2017.
17. Jin B and Robertson KD: DNA methyltransferases, DNA damage repair, and cancer. Adv Exp Med Biol 754: 3-29, 2013.
18. Ahsan MU, Gouru A, Chan J, Zhou W and Wang K: A signal processing and deep learning framework for methylation detection using Oxford Nanopore sequencing. Nat Commun 15: 1448, 2024.
19. Euskirchen P, Bielle F, Labreche K, Kloosterman WP, Rosenberg S, Daniau M, Schmitt C, Masliah-Planchon J, Bourdeaut F, Dehais C, *et al*: Same-day genomic and epigenomic diagnosis of brain tumors using real-time nanopore sequencing. Acta Neuropathol 134: 691-703, 2017.
20. Li H: Minimap2: Pairwise alignment for nucleotide sequences. Bioinformatics 34: 3094-3100, 2018.
21. Capper D, Jones DTW, Sill M, Hovestadt V, Schrimpf D, Sturm D, Koelsche C, Sahm F, Chavez L, Reuss DE, *et al*: DNA methylation-based classification of central nervous system tumours. Nature 555: 469-474, 2018.
22. Maas SLN, Stichel D, Hielscher T, Sievers P, Berghoff AS, Schrimpf D, Sill M, Euskirchen P, Blume C, Patel A, *et al*: Integrated molecular-morphologic meningioma classification: A multicenter retrospective analysis, retrospectively and prospectively validated. J Clin Oncol 39: 3839-3852, 2021.
23. Santana-Santos L, Kam KL, Dittmann D, De Vito S, McCord M, Jamshidi P, Fowler H, Wang X, Aalsburg AM, Brat DJ, *et al*: Validation of whole genome methylation profiling classifier for central nervous system tumors. J Mol Diagn 24: 924-934, 2022.
24. Priesterbach-Ackley LP, Boldt HB, Petersen JK, Bervoets N, Scheie D, Ulhøi BP, Gardberg M, Brännström T, Torp SH, Aronica E, *et al*: Brain tumour diagnostics using a DNA methylation-based classifier as a diagnostic support tool. Neuropathol Appl Neurobiol 46: 478-492, 2020.
25. Ma J, Hong Y, Chen W, Li D, Tian K, Wang K, Yang Y, Zhang Y, Chen Y, Song L, *et al*: High copy-number variation burdens in cranial meningiomas from patients with diverse clinical phenotypes characterized by hot genomic structure changes. Front Oncol 10: 1382, 2020.
26. Wang JZ, Nassiri F, Landry AP, Patil V, Liu J, Aldape K, Gao A and Zadeh G: The multiomic landscape of meningiomas: A review and update. J Neurooncol 161: 405-414, 2023.
27. da Silveira MA, Ferreira WAS, Amorim CKN, Brito JRN, Kayath AS, Sagica FDES and de Oliveira EHC: Meningiomas: An overview of the landscape of copy number alterations in samples from an admixed population. J Oncol 2020: 3821695, 2020.
28. Whitehouse JP, Howlett M, Federico A, Kool M, Endersby R and Gottardo NG: Defining the molecular features of radiation-induced glioma: A systematic review and meta-analysis. Neurooncol Adv 3: vdab109, 2021.
29. Behling F, Barrantes-Freer A, Skardelly M, Nieser M, Christians A, Stockhammer F, Rohde V, Tatagiba M, Hartmann C, Stadelmann C and Schittenhelm J: Frequency of BRAF V600E mutations in 969 central nervous system neoplasms. Diagn Pathol 11: 55, 2016.
30. Kowalewski A, Durślewicz J, Zdrenka M, Grzanka D and Szylberg Ł: Clinical relevance of BRAF V600E mutation status in brain tumors with a focus on a novel management algorithm. Target Oncol 15: 531-540, 2020.
31. Attia AS, Hussein M, Issa PP, Elnahla A, Farhoud A, Magazine BM, Youssef MR, Aboueisha M, Shama M, Toraih E and Kandil E: Association of $BRAF^{V600E}$ mutation with the aggressive behavior of papillary thyroid microcarcinoma: A meta-analysis of 33 studies. Int J Mol Sci 23: 15626, 2022.
32. Zhang S, He S, Zhu X, Wang Y, Xie Q, Song X, Xu C, Wang W, Xing L, Xia C, *et al*: DNA methylation profiling to determine the primary sites of metastatic cancers using formalin-fixed paraffin-embedded tissues. Nat Commun 14: 5686, 2023.
33. Gull N, Jones MR, Peng PC, Coetzee SG, Silva TC, Plummer JT, Reyes ALP, Davis BD, Chen SS, Lawrenson K, *et al*: DNA methylation and transcriptomic features are preserved throughout disease recurrence and chemoresistance in high grade serous ovarian cancers. J Exp Clin Cancer Res 41: 232, 2022.
34. Huntoon K, Toland AMS and Dahiya S: Meningioma: A review of clinicopathological and molecular aspects. Front Oncol 10: 579599, 2020.
35. Hergalant S, Saurel C, Divoux M, Rech F, Pouget C, Godfraind C, Rouyer P, Lacomme S, Battaglia-Hsu SF and Gauchotte G: Correlation between DNA methylation and cell proliferation identifies new candidate predictive markers in meningioma. Cancers (Basel 14: 6227, 2022.
36. Chen CH, Lin YJ, Lin YY, Lin CH, Feng LY, Chang IY, Wei KC and Huang CY: Glioblastoma primary cells retain the most copy number alterations that predict poor survival in glioma patients. Front Oncol 11: 621432, 2021.
37. Yin A, Etcheverry A, He Y, Aubry M, Barnholtz-Sloan J, Zhang L, Mao X, Chen W, Liu B, Zhang W, *et al*: Integrative analysis of novel hypomethylation and gene expression signatures in glioblastomas. Oncotarget 8: 89607-89619, 2017.
38. Matsuda T, Kono T, Taki Y, Sakuma I, Fujimoto M, Hashimoto N, Kawakami E, Fukuhara N, Nishioka H, Inoshita N, *et al*: Deciphering craniopharyngioma subtypes: Single-cell analysis of tumor microenvironment and immune networks. iScience 27: 111068, 2024.
39. Zhao C, Wang Y, Liu H, Qi X, Zhou Z, Wang X and Lin Z: Molecular biological features of cyst wall of adamantinomatous craniopharyngioma. Sci Rep 13: 3049, 2023.
40. Jucá CEB, Colli LM, Martins CS, Campanini ML, Paixão B, Jucá RV, Saggioro FP, de Oliveira RS, Moreira AC, Machado HR, *et al*: Impact of the canonical wnt pathway activation on the pathogenesis and prognosis of adamantinomatous craniopharyngiomas. Horm Metab Res 50: 575-581, 2018.

41. Choudhury A, Magill ST, Eaton CD, Prager BC, Chen WC, Cady MA, Seo K, Lucas CG, Casey-Clyde TJ, Vasudevan HN, *et al*: Meningioma DNA methylation groups identify biological drivers and therapeutic vulnerabilities. Nat Genet 54: 649-659, 2022.
42. Bertero L, Mangherini L, Ricci AA, Cassoni P and Sahm F: Molecular neuropathology: An essential and evolving toolbox for the diagnosis and clinical management of central nervous system tumors. Virchows Arch 484: 181-194, 2024.
43. Lin Y, Dong ZH, Ye TY, Yang JM, Xie M, Luo JC, Gao J and Guo AY: Optimization of FFPE preparation and identification of gene attributes associated with RNA degradation. NAR Genom Bioinform 6: lqae008, 2024.
44. Zhang P, Lehmann BD, Shyr Y and Guo Y: The utilization of formalin fixed-paraffin-embedded specimens in high throughput genomic studies. Int J Genomics 2017: 1926304, 2017.